

RESEARCH ARTICLES

Increasing power generation with enhanced cogeneration using waste energy in palm oil mills

Pisan Booneimsri , Kuskana Kubaha & Chullapong Chullabodhi

Division of Energy Management Technology, School of Energy, Environment and Materials, King Mongkut's University of Technology Thonburi, Bangkok 10140, Thailand

Keywords

Cogeneration, energy efficiency, palm oil mill, power generation, waste energy

Correspondence

Pisan Booneimsri, Division of Energy Management Technology, School of Energy, Environment and Materials, King Mongkut's University of Technology Thonburi, Bangkok 10140, Thailand. E-mail: pisan.emm@gmail.com

Funding Information

No funding information provided.

Received: 13 November 2017; Revised: 28 February 2018; Accepted: 17 April 2018

doi: 10.1002/ese3.196

Abstract

Enhancing power generation using waste energy promotes sustainability. Bio-waste from palm oil mills (POMs) has been used as a renewable energy (RE) source to produce steam and electricity in Thai POMs for decades. Because the amount of generated bio-waste normally exceeds the amount that can be used internally by the POMs, energy-efficient practices in the cogeneration plant, which includes waste heat emitted by sterilization steam venting and the biogas engine in the power plant, are disregarded. However, a government policy that allows operators to sell electricity back to the grid has been enacted, and plant owner's attitudes toward cogeneration have since changed. Increased attention has been focused on fuel conservation and energy-efficiency practices, and this study is a product of that increased interest. This work aims to increase power generation from POMs by integrating waste energy through an improved cogeneration system. A standard 45-t/h fresh fruit bunch (FFB), POM in southern Thailand was selected as a case study. The steam consumption and boiler and turbine efficiency were measured and analyzed along with the data on the engine waste heat, and a power generation model for the POMs was then proposed. The analysis results showed that the surplus electricity can reach 2.834 MW and 4.223 MW with and without crude palm oil (CPO) production, respectively. The operational rate of the cogeneration plant is also suggested to be extended to 7,500 continuous hours per year instead of the 4351 intermittent hours implemented at present.

Introduction

Bio-waste from palm oil mills (POMs) plays a significant role in the sustainable development of several nations. In 2015, the world crude palm oil (CPO) production was 58.84 million metric tonnes (MMT) [1] which was produced via 294 MMT of fresh fruit bunches (FFBs) (based on an oil extraction rate of 20%). Two types of CPO extraction processes are used: dry and wet processing mills [2, 3]. Dry processing mills (or semimechanized mills) are used in rural areas with capacities less than 10 t/h FFB, and these mills use a portion of the heat produced by hot gases from wood burning to extract the oil. The wet process is used by medium and large mills with capacities over 10 t/h FFB [2]. The milling process requires both steam

and hot water for the oil extraction, which generates wastewater known as palm oil mill effluent (POME) [2].

Thailand is the third largest CPO producer worldwide after Malaysia and Indonesia. The plantation and harvesting areas (in 2015) were 751,520 and 684,160 hectares, respectively, in which 11.016 MMT of FFB [4] were produced and mostly fed to wet processing mills (also called wet POMs). In addition, 204 POMs were in operation, including 129 dry and 75 wet processing mills. Wet POMs had a total installed capacity of 2835 t/h FFB [5]. The annual operating hours of the POMs varied from 4000–5000 h because of the FFB production seasonality. Although CPO is the primary product of POMs, the bio-waste byproduct in both solid and liquid form is generated in large quantities and used as an RE resource.

These solid bio-wastes are empty fruit bunches (EFBs), pressed palm fiber (PPF), and palm kernel shells (PKS) with typical residues to product ratios (RPRs) per tonne FFB of 22%, 13.5% and 5.5%, respectively [6]. The amount of liquid waste or POME may range from 0.44 to 1.18 m³/t FFB [2]. PPF is mainly used as fuel for the boiler plant in the POM itself, whereas the PKS is sold and used as an alternative fuel in other industries. EFBs have been the focus of attention as a potential fuel source for power generation. Bazmi *et al.* [7] presented the progress and challenges of utilizing the oil palm biomass for decentralized electricity generation and indicated that the three palm oil leaders Indonesia, Malaysia, and Thailand had the potential to produce 8000, 5000, and 500 GWh, respectively, through high-pressure modern power plants. Mahlia *et al.* [8] conducted a study on the feasibility of using POM waste to support grid power connections in Malaysia. However, using EFB as the fuel for an independent power plant (IPP) has several limitations associated with economic feasibility, and a number of parameters must be considered such as the locations, moisture content in fuel and price [9]. Therefore, an internal use of EFB may be an option.

In addition, POME has been utilized as both a fertilizer and in the production of biogas. Notably, biogas production has gradually increased in several countries [10–15]. Thailand has used biogas fuel in engine power plants for over ten years [15, 16], although the use of waste heat from the engines has been ignored. Recently, Booneimsri *et al.* [17] assessed the waste heat potential of a 1 MW engine power plant, and the result showed that 978.77 kW of waste heat (36.67% of the energy input) was recovered and could be utilized.

Wet POM employs a steam boiler that generates steam at typically 2.1 MPa and 235°C and supplies a back pressure steam turbine (BPST) to drive a generator for power generation. The exhaust steam from the turbine is fed into the POM at 0.3 MPa and 145°C. Generally, the generated amounts of electricity and steam are sufficient for the milling process. The power and steam requirements to process one tonne of FFB vary from 15–20 kW and 500–700 kg, respectively [18–20]. Because the cogeneration efficiency of POMs is moderate [19, 20], several researchers have proposed improving the cogeneration efficiency. Nasrin *et al.* [20] assessed the cogeneration performance and the potential to export the surplus generated power. The authors showed that most of the boilers and turbines used in POMs have moderate efficiencies of less than 80% and 35%, respectively, whereas the potential excess electricity for export is 113 kW for a 20 t/h FFB mill to 900 kW for a 54 t/h FFB mill. Husain *et al.* [21] analyzed biomass-based cogeneration to enhance its efficiency, and their report claimed that steam boilers and turbines used

in POMs had low thermal efficiencies and suggested that the use of condensing turbines could increase the power output by 60%.

Aziz and Kurniawan [22] proposed an integrated palm waste utilization system for power generation that consisted of EFB syngas power generation, POME biogas power generation, and organic Rankine cycle (ORC) power generation driven by the engine flue gas. In this system, waste heat circulation technology is employed for the EFB drying process to enhance the energy efficiency, and the authors showed that potential for total net power generation is 8.5 MW (at 10 t/h EFB) and the efficiency was 30.4%.

Exhausted steam from the turbine is received by a back pressure vessel (BPV) and distributed to the palm oil milling process, primarily to the sterilization and heating processes. The sterilization process is the highest steam consumer and account for 35–45% of the total steam generated. Because the operation of the units causes the steam pressure to fluctuate, and BPST should be held constant at 0.3 MPa, intermittent venting of high-pressure steam is unavoidable. The amount of steam loss caused by steam venting is reported as 43–56% of the steam feed or 20–23% of total steam produced [2, 23–25]. Mohd Halim Shah *et al.* [23, 24] investigated the steam pressure swing caused by the sterilizing cycle and proposed the use of a steam accumulator to reduce the steam pressure fluctuations. However, the study is not concerned with sterilization steam loss from steam venting.

Several studies have focused on waste energy potential and cogeneration enhancement in POMs and presented various approaches. However, the previous findings have not been consolidated into a single model. Thailand's integrated energy policies [26] have encouraged waste energy utilization and energy-efficiency improvements to achieve national goals and satisfy global energy and environmental agreements [27]. These policies include the Thailand Power Development Plan (PDP 2015), the Thailand Alternative Energy Development Plan (AEDP 2015), and the Thailand Energy Efficiency Development Plan (EEDP 2015).

This paper aims to increase power generation in POMs by integrating the harnessed waste energy, including sterilization vented steam, engine waste heat and EFB through an improved cogeneration model. A new paradigm for sustainable electricity production in POMs is proposed, and a Thai POM is used as a case study. Technical barriers to and energy policies in support of the scheme are also discussed.

Methodology

This study has been conducted in three main stages: the selection of a POM for case study, the field data measurements, collections and surveys, and the data calculations and

analysis. The selected POM is located in southern Thailand in Surat Thani Province, which is in the most concentrated palm oil plantation areas. The mill operates using a standard wet process with a 45 t/h FFB capacity. Biomass-based cogeneration is performed to produce electricity and steam used in the milling process, whereas biogas produced from POME is used as fuel for a gas engine power plant.

To measure and record data at the site, insertion vortex flow meters (M23 type with temperature sensor compensation) were used to measure the steam and water flow capacity. Pressure and temperature transmitters were installed to monitor the steam inlet and outlet conditions, whereas a power meter was connected to the generator to measure the steam turbine's power generation. All measured data were monitored and recorded by an ES-749 utility metering flow computer. The steam and power generation of the cogeneration plant was continuously measured and recorded for 24 h. For the steam consumption of the CPO process, the cyclical peak steam demand of the sterilization process was measured and recorded for 8 h to obtain the steam consumption pattern for analysis, whereas the regular steam usage in the heating process was measured hourly. The information obtained was used to calculate and analyze, the steam boiler and turbine efficiency, the steam cogeneration efficiency, the engine power plant efficiency and its waste heat potential, and the amount of steam vented by the sterilization process.

The FFB feeding capacity is recorded by the mill, whereas the PPF and EFB generation were calculated from RPR. The engine power plant data (recorded by SCADA) were taken from the factory and used to determine the engine power plant efficiency and waste heat potential. For energy analysis and further calculations, the following assumptions are used:

- the LHV values of PPF, EFB, and PKS are 11.4 (at 38.50% moisture), 7.24 (at 58.60% moisture), and 16.9 (at 12% moisture) MJ/kg, respectively [28], the moisture contents are based on a wet basis (wb):
- the RPR values of PPF, EFB, and PKS per tonne FFB are 0.135, 0.22, and 0.055, respectively [6]:
- the LHV of biogas is 5.833 kWh/Nm³ (based on 62% CH₄, 15.6°C, and 101.2 kPa) [29]:
- the proposed steam boiler efficiency is 80% (NCV):
- the steam pressure and temperature are 4.8 MPa and 470°C, respectively:
- the isentropic efficiencies of the extraction and condensing turbine are assumed to be 75 and 77%, respectively:
- the mechanical and generator efficiencies are 98 and 95%, respectively:
- the extraction and condensing steam pressure are 0.3 MPa and -0.0863 MPa, respectively;

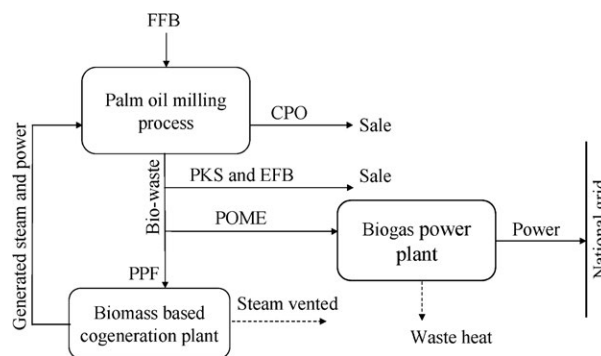


Figure 1. Diagram of POM processes under the study.

- the makeup water and desuperheating water temperature are 30°C:
- the steam condensation of the process is saturated liquid at 100°C, which is not reused:
- the boiler blowdown and thermal and pressure loss via piping are neglected.

A diagram of the POM processes is shown in Figure 1.

System analysis

Plant general description

The selected factory is a wet POM at 45-t/h FFB, and is located in Suratthani Province in southern Thailand. The mill consumes 200,805 tonnes FFB annually and operates for approximately 4351 h. The POM consists of three main sections: a palm oil milling plant, a steam cogeneration plant, and a biogas power plant. The palm oil milling process includes sterilization, threshing, digestion, extraction, clarification, fiber and nut separation, and kernel drying. These processes generate large amounts of bio-waste byproducts, including: PPF, EFB, PKS, and POME. PPF is primarily used as a boiler fuel for the steam cogeneration plant, which produces sufficient steam and electricity for factory use. EFB and PKS are sold to other plants or traders, whereas POME is used as a feedstock to produce biogas, which is used as fuel in the engine power plant under the nation's RE scheme. The post-treatment of wastewater is either drained into a public drainage ditch or pumped to the oil palm plantation area nearby. Figure 2 shows the POM processes used in this study, and the operation of each section is illustrated below.

Palm oil milling process description

The steam and electricity generated from the cogeneration plant are dedicated to the palm oil milling process at state 4 and state 12, respectively. The steam is mainly consumed by the sterilization and heating processes at

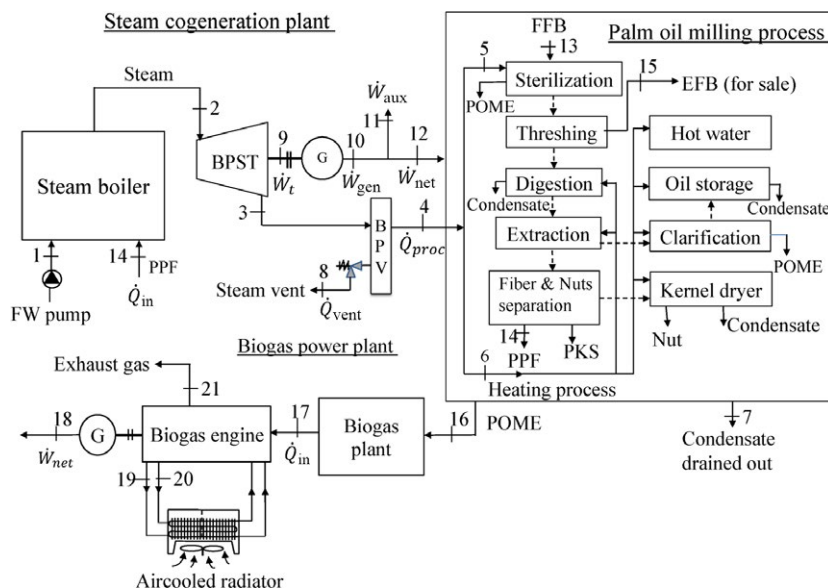


Figure 2. Current process diagram of selected POM.

state 5 and 6 (Fig. 2). Because the most steam demand and loss (vented steam) occur at the sterilization process, the characteristics of the sterilization process were examined. Four sterilizers are observed in the POM, and FFB fed into each sterilizer (stage 13) sequentially. Steam from the BPV is systematically directly injected into the sterilizer to create the appropriate FFB properties for oil extraction. Three types of sterilization methods are employed: single, double, and triple peak cycles. The operation of each cycle depends on the FFB conditions, although the triple peak cycle is the most often used [23]. The cycles are controlled by a programmable logic controller (PLC). Figure 3 shows the typical triple peak sterilization cycle and its operational sequence [23]. Because sterilization is a batch operation, steam consumption is intermittent and peaks at the beginning of the shooting stage, which causes the steam pressure to drop suddenly. After the steam replenishment into the sterilizer is complete, the steam pressure gradually rises and vents into the atmosphere at 0.302 MPa (state 8) to complete the cycle.

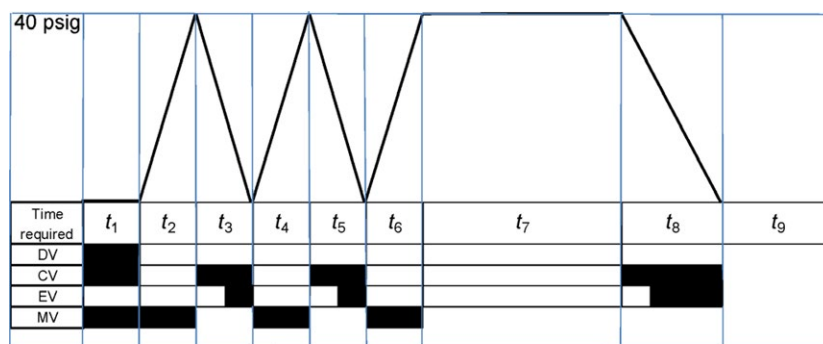
In addition, steam is supplied to heating processes that consumes steam steadily, including the kernel drier, clarification, extraction, the CPO tank, digestion, and the hot water tank. The sterilized FFBs contain fruits and bunch stalks, and they are separated by the threshing process. The bunch stalks without fruits are called EFBs and stored for sale at stage 15, whereas the ripped fruits are cooked in the digestion process at 90–95°C. The cooked fruits are squeezed by screw presses and oil is expelled in the extraction process. The extracted oil is sent to clarification process to remove contaminants, such as water and other

impurities via settling, centrifuging, and drying techniques. The purified CPO is stored in CPO tanks and warmed by steam. The pressed fruits are called cake, which contains PPF and nuts.

The PPF and nuts are separated by a fiber and nut separation process. Nuts are composed of PKS and kernels, are separated. The separated PKS are sold for use as an alternative fuel for general industries. In addition, the kernel (which contains palm kernel oil, PKO) is dried in a drier and sold to a kernel crushing plant for further processing, whereas the PPF is used as boiler fuel in the steam cogeneration plant (state 14). The condensate of the heating process is drained at state 7 and not reused, and the wastewater or POME from the processes (mainly from the sterilization and clarification process) is collected and sent to the biogas power plant at state 16.

Steam cogeneration plant operation

The steam and electricity used in the POM are generated from the steam cogeneration plant which mainly consists of a steam boiler and BPST. The steam boiler is the conventional type (water tube and fixed grate combustion) with a designed steam capacity of 22.7 tonnes/h at 2.1 MPa and 237°C (superheated steam) using the PPF as fuel. The BPST is a radial-flow single-stage type and is designed for a 1080 kW full load (FL) at 24.58 kg/kWh and a specific steam rate (SSR) at 2.1 MPa and 230°C at the turbine inlet and 0.3 MPa and 145.4°C steam exhaust point. The steam turbine cogeneration simultaneously transforms the fuel's chemical energy to thermal output (steam) and electricity. The feedwater (FW at 95°C) from



Open DV = Deaeration valve EV = Exhaust valve
 Close CV = Condensate valve MV = Main (Steam) valve

Ideal steaming step and time for triple peak sterilization cycle (Sivasothy et al., 1990) [79]

Sequence step	Time (Min.)	Valve status			
		Main steam valve	Exhaust valve	Deaeration valve	Condensate valve
1 Deaeration	5	o	x	o	x
2 First peak pressure built-up	8	o	x	x	x
3 Exhaust	3	x	o	x	o
4 Second peak pressure built-up	8	o	x	x	x
5 Exhaust	3	x	o	x	o
6 Third peak pressure built-up	8	o	x	x	x
7 Full pressure steaming	30	o	x	x	x
8 Exhaust	5	x	o	x	o
9 Discharging and charging	10	x	x	x	x
10 Idle time before next step	10	x	x	x	x
Cycle time	90				

Figure 3. Ideal triple peak sterilization cycle [23].

the hot water tank is fed into the boiler by a feedwater pump at state 1 (Fig. 2), whereas the fuel (PPF) from the process is supplied at state 14. The fuel’s chemical energy is changed to heat by combustion in the boiler furnace and then is transferred to the water to evaporate as steam. The high-pressure steam generated is supplied to the BPST at state 2, where the thermal energy (steam) is transformed into mechanical work via expansion in the turbine (shaft work at state 9) and converted into electrical work by a generator at state 10. The generated power from the generator feeds into two sections: the first is the cogeneration plant to drive the auxiliaries (state 11) and the second is the factory use (state 12). The low-pressure steam (usually 0.3 MPa) is exhausted from the turbine at state 3 and received by the BPV, which is temporary steam storage, and then distributed to the palm oil milling process at state 4. Figure 4 shows the T-S diagram of the current cogeneration with the BPST.

Biogas power plant operation

The biogas power plant consists of three subsystems: biogas production, biogas cleaning, and biogas power generation. Figure 5 shows the schematic diagram of the biogas power plant.

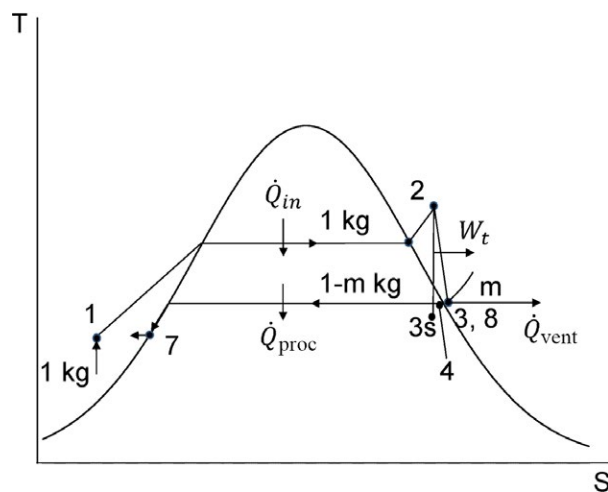


Figure 4. T-S diagram of the current cogeneration plant.

POME collects in an equalization tank and is fed into a digester tank where biogas is generated by an anaerobic digestion technique using a continuously stirred tank reactor (CSTR). The biogas produced consists mainly of 55–70% methane (CH_4), 30–45% carbon dioxide (CO_2), and small traces of other gases, moisture, and hydrogen sulfide, and it has a heating value of 18–24 MJ/m³ [29].

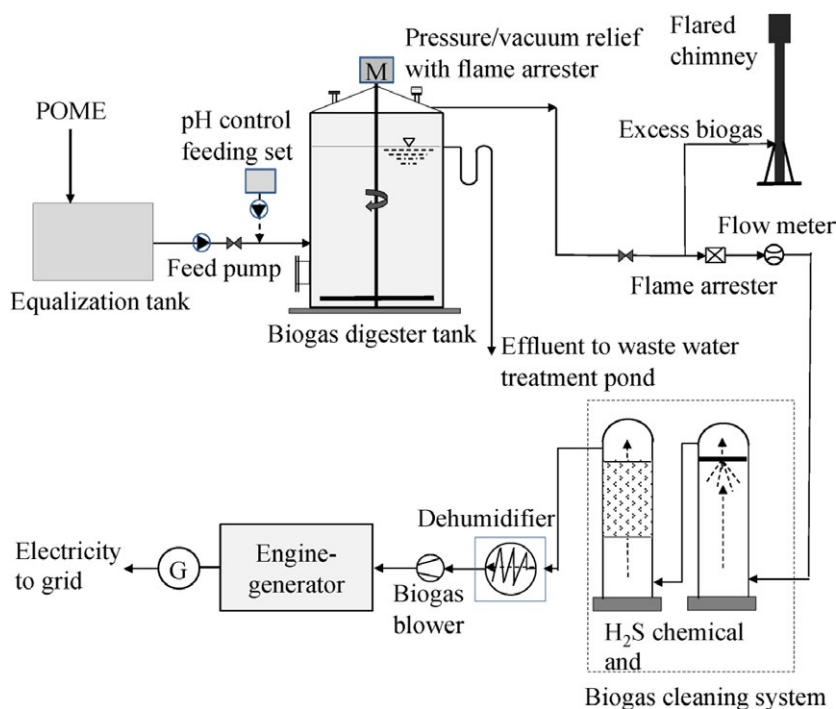


Figure 5. Biogas power plant diagram of the POM.

Because the contaminant gases affect the engine performance, particularly, hydrogen sulfide, which is harmful to the engine parts, they need to be removed before use [29]. Water scrubbers and a dehumidifier are installed to clean the biogas to remove the hydrogen sulfide, carbon dioxide, and moisture. Because of environmental and safety issues, a flared chimney is provided to convert the methane to carbon dioxide by combustion when the biogas amount is excessive.

The processed biogas is used as engine fuel. The engine is installed as a VSPP, and it is a spark-ignition type (SI engine) that is rated for 1063 kW, but usually operates at 1000 kW. The produced biogas feeds into the engine at state 17 (Fig. 2.). The fuel's chemical energy is transformed into electricity through fuel combustion and gas expansion in the engine cylinders to create a mechanical rotation, which is converted into electricity by a generator (state 18). Despite the efforts to convert the combustion heat to mechanical work, a certain amount of heat loss is unavoidable and becomes waste heats to the environment. The major sources of waste heats are from the exhaust gas and the engine cooling water system, whereas minor heat losses are dissipated as radiation, from the generator and through other avenues.

Two engine cooling water closed circuits are included: the low-temperature (LT) and high-temperature (HT) circuits (state 19 and 20). The LT circuit absorbs the heat of the engine aftercooler, and the HT circuit absorbs

the engine jacket heat, lubrication and intercooler. The heat absorbed is dumped into air-cooled radiators to maintain proper coolant temperature at 50–52.3°C and 70–90°C for the LT and HT circuits, respectively. In addition, the high-temperature exhaust gas (at 487°C) escapes to the atmosphere at state 21 as thermal pollution. Figure 6 shows the Sankey diagram of the energy flow and losses of the 1.063 MW engine power plant.

Proposed an enhanced cogeneration system

Increasing the steam pressure and temperature is recommended to improve the Rankine cycle efficiency [30]. The proposed model uses an extraction-condensing steam turbine (ECST) with a steam rating of 4.8 MPa and 470°C. The steam boiler capacity is 6.388 kg/sec (23 t/h), which is nearly equivalent to the existing capacity to ensure that the boiler can handle the peak demand. The results of the energy analysis of the current POM were adapted to the proposed model. The model is intended to improve the power generation in the POM with and without CPO production by using PPF and EFB as boiler fuels and utilizing wasted energy, i.e., vented steam and engine waste heat. Therefore, high-pressure steam boiler and the ECST were applied to harness the wasted energy.

The ECST can manage a broader range of steam demand variations compared with the BPST, which requires a close match between the power and steam requirements

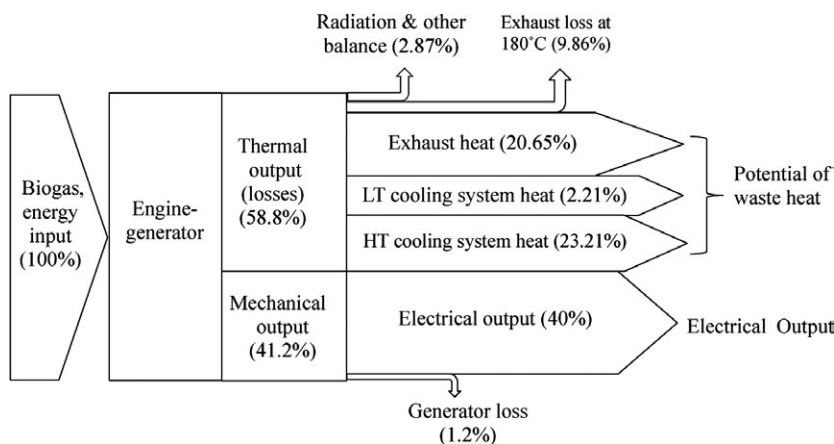


Figure 6. The energy flow of 1.063 MW engine-generator.

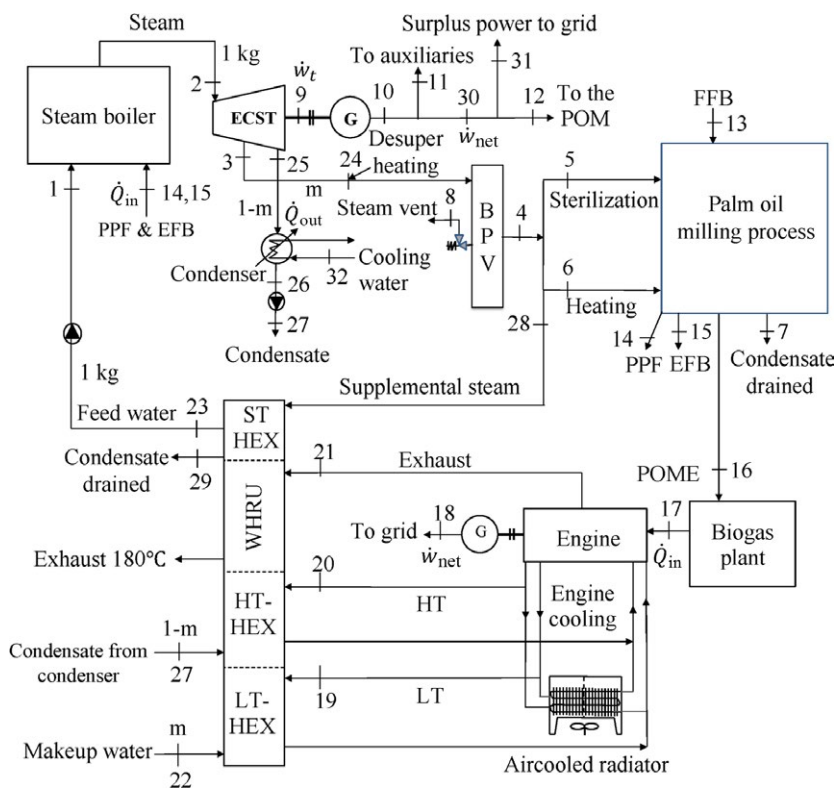


Figure 7. Proposed model of enhanced power generation in POMs.

[31]. In addition, the ECST has great flexibility in operating range during the CPO production, and it can produce power without CPO production, which extends the cogeneration plant operation continuously throughout the year as opposed to the usual intermittent operation. Harnessing and utilizing the waste energy through the improved cogeneration process increases the power generating capacity and energy efficiency. The proposed model is shown in Figure 7.

The PPF and EFB feed into the boiler at state 14 and 15. The PPF is primarily used as fuel during CPO production, whereas the EFB was planned for use without the CPO production. The electrical efficiency of the SI engine-generator may vary from 28–42% [32]. The remainder of the energy is changed into waste heat in the exhaust gas and engine cooling systems. The waste heat is utilized to increase the temperature of the boiler FW through heat exchangers, which reduces the process steam

used. The makeup water at state 22 (design to be 30°C) and the condensate from the condenser at state 27 feed into the LT and HT heat exchanger (LT-HEX and HT-HEX) to extract the heat of the LT and HT circuit (state 19 and 20), respectively. The mixed water (makeup water and condensate) from the HT-HEX flows through the waste heat recovery unit (WHRU) to absorb the exhaust heat (state 21). Nevertheless, supplemental heat may require increasing the FW temperature to the designed temperature (105°C). The steam heat exchanger (ST-HEX) meets for this requirement by supplying steam at state 28.

The high-temperature FW at state 23 is fed into the boiler (state 1). The high-pressure steam generated from the boiler is supplied into the ECST at state 2. The steam outlet of the turbine is divided into: an extraction port (state 3) and a condensing port (state 25). The extraction steam rate will vary with the process demand (state 4). Specifically, when the sterilization steam demand decreases, the steam pressure at the BPV increases and the steam extraction rate is throttled, and vice versa. The remaining steam from extraction will pass through the turbine to the condenser without vented steam at state 8. Typically, the steam extracted from the turbine is superheated steam; consequently, desuperheating water is needed to make saturated steam (state 24) before supplying the processes (state 4).

The condensing steam from the turbine (state 25) condenses in a condenser and the heat is rejected to the cooling water (state 32). The condensate from the condenser (state 26) is pumped into the HT-HEX at state 27. Electricity (state 9) is generated via the extraction and condensing turbine combination; the gross power (state 10) is consumed by the auxiliaries in the cogeneration plant (state 11) and in factory use (state 12), and the surplus power is exported to the grid (state 31). When CPO production is not performed, the cogeneration plant continues to operate, although most of the generated steam will pass out the turbine to the condenser, and become dedicated to power generation for the grid. The collected EFB during CPO production is used for fuel in this mode. Figure 8 shows a T-S diagram of the cogeneration plant cycle with the proposed extraction-condensing turbine.

Energy analysis

The first law of thermodynamics is a conventional thermodynamic analysis, which is typically used to assess and compare systems [33]. In the study, the first law of thermodynamics with a close system steady-flow process is applied to evaluate the systems' energy efficiencies, whereas the kinetic and potential energy changes are negligible.

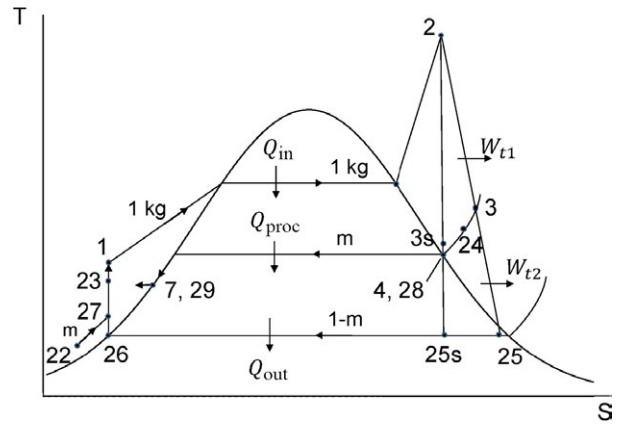


Figure 8. T-S diagram of enhanced cogeneration system.

Steam turbine cogeneration plant

The steam boiler and turbine efficiency in the cogeneration plant (Fig. 2 illustrates the states) can be expressed as follows:

$$\eta_b = \frac{\dot{E}_{out}}{\dot{E}_{in}} = \frac{\dot{m}_2 * (h_2 - h_1)}{\dot{m}_{14} * LHV_{PPF}} \quad (1)$$

where η_b is the boiler efficiency; \dot{E}_{in} and \dot{E}_{out} are the energy input and output of the steam boiler, respectively, in kW; \dot{m}_2 and \dot{m}_{14} are the mass flow rate of the steam generated by the boiler and the mass flow rate of the feed fuel, respectively, in kg/sec; h_1 and h_2 are the specific enthalpy of the boiler feedwater and the generated steam, respectively, in kJ/kg; and LHV_f is the lower heating value (LHV) of the PPF in kJ/kg. Because the fuel moisture is usually in a vapor state in the exhaust gas, the latent heat of water vapor is ignored; thus, the LHV is applied [34]. Because the fluid experiences friction in the turbine, the steam expansion process is irreversible and the entropy of the fluid increases. The isentropic efficiency of the turbine is then defined as follows:

$$\eta_{t-isen} = \frac{\dot{W}_9}{\dot{W}_{is}} = \frac{\dot{m}_2 (h_2 - h_3)}{\dot{m}_2 (h_2 - h_{3s})} \quad (2)$$

where η_{t-isen} is the turbine isentropic efficiency; \dot{w}_9 and \dot{w}_{is} are the turbine shaft actual and isentropic power output, respectively, in kW. The isentropic enthalpy can be determined from the exit pressure and the exit entropy (at the same point as the inlet entropy). In addition, h_3 and h_{3s} are the enthalpy of the exhausted steam in the actual and isotropic case, respectively, in kJ/kg. The cogeneration plant efficiency can be expressed as the ratio of the net power output (\dot{Q}_{net}, kW) combined with the process heat utilized (\dot{Q}_{proc}, kW) minus the vented steam (\dot{Q}_{vent}, kW) to the energy input, as follows:

$$\eta_{\text{cogen-st}} = \frac{\dot{W}_{\text{net}} + \dot{Q}_{\text{proc}} - \dot{Q}_{\text{vent}}}{\dot{E}_{\text{in}}} = \frac{\dot{W}_{12} + \dot{m}_4 * (h_4 - h_7) - \dot{m}_8 * h_8}{\dot{m}_f * \text{LHV}_f} \quad (3)$$

where $\eta_{\text{cogen-st}}$ is the steam cogeneration efficiency in %; \dot{m}_4 and \dot{m}_8 are mass flow rates of the process and vented steam, respectively, in kg/sec; h_4 , h_7 , and h_8 are specific enthalpies of the process steam, condensate, and vented steam, respectively, in kJ/kg; \dot{w}_{net} is the net power output in kW after mechanical and generator loss of the turbine along with the auxiliary power consumption of the cogeneration plant are considered; and \dot{w}_{12} is the factory power consumed in kW. Thus, \dot{w}_{12} is equal to \dot{w}_{net} in this case, and can be expressed as follows:

$$\dot{w}_{\text{net}} = \dot{w}_{10} - \dot{w}_{11} = (\dot{w}_9 * \eta_{\text{mech}} * \eta_{\text{gen}}) - \dot{w}_{11} \quad (4)$$

where η_{mech} and η_{gen} are the mechanical and generator efficiency of the turbine and generator, respectively, in %; \dot{w}_{10} is the gross power output of the generator in kW, and \dot{w}_{11} is the power consumed to drive the auxiliaries of the cogeneration plant in kW.

Waste steam from the sterilization steam vent

The quantity of vented sterilization steam is a significant source of waste steam for the POM (Fig. 2 illustrates state8), and can be determined from the following equation:

$$\dot{m}_8 = \dot{m}_3 - \dot{m}_4 = \dot{m}_3 - \dot{m}_5 - \dot{m}_6 \quad (5)$$

where \dot{m}_3 , \dot{m}_5 , \dot{m}_6 , and \dot{m}_8 are the steam mass flow rates of the turbine exhaust, sterilization process, heating process and the vented steam, respectively, in kg/sec.

Engine-based power plant

Based on an engine-generator operating as a power plant, the electrical efficiency is defined as a ratio of the net power output of the generator to the energy input (Fig. 2 illustrates the state):

$$\eta_{\text{el}} = \frac{\dot{w}_{18}}{\dot{Q}_{\text{in}}} = \frac{\dot{w}_{18}}{\dot{V}_{\text{BG}} * \text{LHV}_{\text{BG}}} \quad (6)$$

where η_{el} is the electrical efficiency of the engine-generator, \dot{w}_{18} is the net power output of the generator in kW; \dot{Q}_{in} is the energy input of the engine in kW; \dot{V}_{BG} is the volumetric flow rate of biogas fuel in Nm³/h; and LHV_{BG} is the LHV of biogas in kWh/Nm³.

Enhanced cogeneration system

Steam generation at state 2 is constant, although the steam consumed in the palm oil milling process fluctuates because of sterilization (state 5), which causes the extraction steam rates to change accordingly (Fig. 7 shows the states). Thus, the steam consumption in the palm oil milling process can be grouped into maximum, minimum, and average cases. Therefore, the inlet steam capacity, extraction, and condensing steam rate of the ECST at state 2, 3, and 25 will relate to these equations:

$$\dot{m}_2 = \dot{m}_{3,\text{max}} + \dot{m}_{25,\text{min}} \quad (7)$$

$$\dot{m}_2 = \dot{m}_{3,\text{min}} + \dot{m}_{25,\text{max}} \quad (8)$$

$$\dot{m}_2 = \dot{m}_{3,\text{avg}} + \dot{m}_{25,\text{avg}} \quad (9)$$

where \dot{m}_2 is the constant steam generated by the boiler in kg/sec; $\dot{m}_{3,\text{max}}$, $\dot{m}_{3,\text{min}}$, and $\dot{m}_{3,\text{avg}}$ are the maximum, minimum, and average of the extracted steam rate of the turbine at state 3, respectively, in kg/sec; and $\dot{m}_{25,\text{min}}$, $\dot{m}_{25,\text{max}}$, and $\dot{m}_{25,\text{avg}}$ are the minimum, maximum, and average of the condensing steam rate of the turbine at state 25, respectively, in kg/sec. In addition to the variations of the steam extraction rate, the steam extracted is a superheated steam; thus, desuperheating water must be mixed with the superheated steam at state 24 to produce saturated steam. Consequently, the extracted steam rate of the turbine is equal to the steam consumed in the heating and sterilization processes minus the required desuperheating water, which is given as follows:

$$\dot{m}_{3,\text{max}} = (\dot{m}_6 + \dot{m}_{5,\text{max}}) - \dot{m}_{24,\text{max}} \quad (10)$$

$$\dot{m}_{3,\text{min}} = (\dot{m}_6 + \dot{m}_{5,\text{min}}) - \dot{m}_{24,\text{min}} \quad (11)$$

$$\dot{m}_{3,\text{avg}} = (\dot{m}_6 + \dot{m}_{5,\text{avg}}) - \dot{m}_{24,\text{avg}} \quad (12)$$

where \dot{m}_6 is the constant heating process steam consumed in kg/sec; $\dot{m}_{5,\text{max}}$, $\dot{m}_{5,\text{min}}$ and $\dot{m}_{5,\text{avg}}$ are the maximum, minimum, and average of the sterilization steam demand, respectively, in kg/sec. The term $\dot{m}_{5,\text{max}}$ applies when three sterilizers are in the cooking stage and the last sterilizer is in a shooting stage at the same time; the term $\dot{m}_{5,\text{min}}$ is a condition in which only one sterilizer is cooking and the other sterilizers are idle; and the term $\dot{m}_{5,\text{avg}}$ is the average steam required for the sterilization process. In addition, $\dot{m}_{24,\text{max}}$, $\dot{m}_{24,\text{min}}$, and $\dot{m}_{24,\text{avg}}$ are the maximum, minimum, and average mass flow rates required for desuperheating water, respectively, in kg/sec. These mass flow rate requirements depend on the superheated steam condition, the desuperheating water temperature and the condition of the required saturated steam, which can be determined from the following heat and mass balance equations:

$$\dot{m}_{24,\max} = \frac{\dot{m}_{3,\max} * (h_3 - h_4)}{(h_4 - h_{24})} \quad (13)$$

$$\dot{m}_{24,\min} = \frac{\dot{m}_{3,\min} * (h_3 - h_4)}{(h_4 - h_{24})} \quad (14)$$

$$\dot{m}_{24,\text{avg}} = \frac{\dot{m}_{3,\text{avg}} * (h_3 - h_4)}{(h_4 - h_{24})} \quad (15)$$

where h_3 , h_4 , and h_{24} are the enthalpy of the extracted superheated steam, the saturated steam at the extracted pressure and desuperheating water, respectively, in kJ/kg. The extraction and condensing steam temperature at state 3 and 25 can be determined using the Mollier diagram when the enthalpy of the extraction and condensing steam are known, which can be determined via Equation (2), whereas the heat load of condensing steam rejected in the condenser can be calculated as follows:

$$\dot{Q}_{\text{out}} = \dot{m}_{25} * (h_{25} - h_{26}) \quad (16)$$

where \dot{Q}_{out} is the condenser heat load in kW; and h_{25} and h_{26} are the enthalpy of the inlet steam and the outlet condensate of the condenser, respectively, in kJ/kg. The shaft power output of the ECST for any case (maximum, minimum, and average) is a combination of the work generated by the extraction and condensing steam:

$$\dot{w}_g = \dot{w}_{i1} + \dot{w}_{i2} = \dot{m}_3 * (h_2 - h_3) + \dot{m}_{25} * (h_2 - h_{25}) \quad (17)$$

where \dot{w}_g is the total shaft power output of the ECST in kW; and \dot{w}_{i1} and \dot{w}_{i2} are the shaft power generated by the extraction and condensing steam respectively, in kW. Considering the mechanical and generator efficiencies, the net power output at the generator is same as in Equation (4), although in this model, the net power output is fed into two paths, factory use and exported to the grid:

$$\dot{w}_{\text{net}} = \dot{w}_{30} = \dot{w}_{31} + \dot{w}_{12} \quad (18)$$

where \dot{w}_{30} and \dot{w}_{31} are the net power and surplus power, respectively, in kW. The thermal efficiency of the proposed model both with and without CPO production can be evaluated as follows:

$$\eta_{\text{th}} = \frac{\dot{w}_{\text{net}} + \dot{Q}_{\text{proc}}}{\dot{Q}_{\text{in}}} = \frac{\dot{W}_{\text{net}} + \dot{m}_4 * (h_3 - h_7)}{\dot{m}_f * \text{LHV}_f} \quad (19)$$

where η_{th} is the thermal efficiency of the cogeneration system in % and the \dot{Q}_{proc} is neglected when CPO is not produced.

In this study, the utilization of engine waste heat is considered cogeneration. Therefore, the efficiency of the engine-based cogeneration is determined as follows:

$$\eta_{\text{cogen-en}} = \frac{\dot{W}_{\text{net}} + \dot{Q}_{\text{WHU}}}{\dot{V}_f * \text{LHV}_f} \quad (20)$$

where $\eta_{\text{cogen-en}}$ is the efficiency of the engine-based cogeneration and \dot{Q}_{WHU} is the actual waste heat utilization for a fully loaded engine in kW. Because the actual running of the engine is lower than FL, the waste heat utilization factor must be corrected, which can be written as follows:

$$\begin{aligned} \dot{Q}_{\text{WHU}} &= (\dot{Q}_{\text{LT}} * \text{PAF} + \dot{Q}_{\text{HT}} * \text{PAF} + \dot{Q}_{\text{exh}} * \text{PAF}) * \epsilon \quad (21) \\ &= (\dot{Q}_{19} + \dot{Q}_{20} + \dot{Q}_{21}) \end{aligned}$$

where \dot{Q}_{LT} , \dot{Q}_{HT} and \dot{Q}_{exh} are the heat generated at FL of the LT and HT circuits and exhaust gas, respectively, in kW; ϵ is the heat exchanger effectiveness, which is assumed to be 0.85; *PAF* is a performance adjustment factor [34] and represents is the ratio of waste heat generated at any load to the waste heat generated at FL in %; and \dot{Q}_{20} and \dot{Q}_{21} are the actual waste heat utilization of the LT, HT, and exhaust circuits, respectively in kW. The *PAF* of each load can be determined by the interpolation method as follows:

$$\text{PAF} = 1 - \left[1 - \frac{(\dot{Q}_{\text{PL}})}{\dot{Q}_{\text{FL}}} \right] * \left[\frac{\Delta \text{FL}_{\text{AL}}}{\Delta \text{FL}_{\text{PL}}} \right] \quad (22)$$

where \dot{Q}_{FL} and \dot{Q}_{PL} are the waste heat generated with a FL and partial load (PL), respectively in kW; and are the percentage differential between the FL and the actual load (AL) and the FL and the PL, respectively, in %. The waste heat of the FL and PL are provided by the engine manufacturer. Because waste heat is used to increase the FW temperature, the elevated FW temperature of each stage can be simplified by the heat balance equation as follows:

$$\dot{Q} = \dot{m}_w * C_{p,w} * \Delta T_w \quad (23)$$

where, \dot{Q} is the heat transfer rate of the supplied heat in kW, \dot{m}_w is the mass flow rate of water that absorbs the heat in kg/sec, $C_{p,w}$ is the specific heat of water at constant pressure in kJ/kg°C and T_w is the temperature difference of the inlet and exit FW in °C. The inlet and exit FW temperature are designed to be 30°C and 105°C, respectively. If the exit FW temperature of the WHRU is lower than the design temperature, the supplementary steam (state 28) will be supplied to the ST-HEX to achieve the desired temperature. The supplementary steam requirement can be calculated from the mass and heat balance:

$$\dot{m}_{28} = \frac{(\dot{m}_{22} + \dot{m}_{27}) * C_{p,w} * (105 - T_{e,\text{WHRU}})}{(h_{g,28} - h_{f,28})} \quad (24)$$

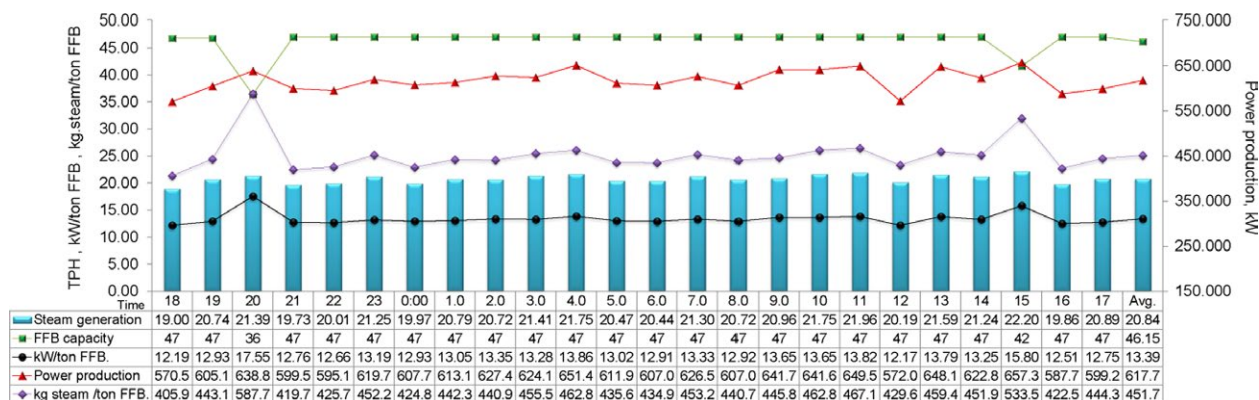


Figure 9. Steam and power consumption profile of the POM.

where \dot{m}_{28} is the mass flow rate of the required supplementary steam in kg/sec, and $h_{g,28}$ and $h_{f,28}$ are the enthalpy of the saturated steam and condensate at 100°C, respectively in kg/sec.

Results and Discussions

Current system

The measured and collected data for the cogeneration plant operation, process steam consumption, and engine power plant operation were analyzed and evaluated to adapt the obtained data to the proposed model.

Energy consumption and cogeneration efficiency

The steam and power consumption profile for the POM is shown in Figure 9. The steam boiler was operated at full capacity between 19 and 22.2 t/h, and its average steam generation and pressure are 20.85 t/h (5.791 kg/sec) and 2.024 MPa, respectively. The turbine generated 571–657 kW power, with 618 kW generated on average. The calculated ratios of power and steam consumption per tonne FFB were 13.39 kW and 451.7 kg, respectively, which are slightly lower than other reported values (15–20 kW and 500–700 kg [15, 20]). The calculated boiler efficiency was 72.16% on NCV.

The steam turbine operational data are shown in Figure 10, and this report is the first to present such data in this field. The turbine operates at 57.2% of its rated power, and its isentropic efficiency and average SSR were calculated as 36.54% and 33.76 kg/kW, respectively. The calculated SSR is close to the SSR curve of the turbine manufacturer, and the turbine consumes steam at 137% of its rated FL (25.58 kg/kW). Because the turbine is primarily designed to match the steam and power

requirement, its efficiency is secondary. The turbine estimated efficiency results are consistent with those given by other studies [21, 22]. The calculated cogeneration efficiency was 36.05%, which is moderate. The POM generated bio-waste far exceeded the demand, the turbine efficiency was low, and sterilization steam was vented; however, these factors were disregarded, which resulted in inefficient cogeneration. The power consumed to drive the cogeneration auxiliaries was 88.05 kW (state 11), which represented 14.25% of the generator output.

The sterilization steam consumption profile is shown in Figure 11. This profile confirms that steam fluctuations occurred. Figure 11A shows the variations in the steam demand, pressure and steam venting of the sterilization process, and Figure 11B shows the sequences of the four sterilizer operations, which were observed while the steam amounts were being recorded.

The vented steam represents a significant energy loss and was estimated 1.354 kg/sec (state 8) or 23.38% of the total steam production, which is in the same range as another study [30]. Thus, the actual average steam required for the sterilization was 2.104 kg/sec (state 5). The steam vented during the sterilization process is a characteristic of batch processing. The sterilization steam demand increased immediately from less than 2 t/h up to 12 t/h in 7 min during the shooting stage, while the steam pressure declined quickly from 3 bar to 1 bar at the same time. After the steam was completely replenished in the sterilizer and cooking was underway, the steam demand gradually decreased while the steam pressure steeply increased until it was vented at 3.02 bar. The behavior was cyclical and similar to another study [24]. The average calculated steam consumptions of the cooking and shooting stages were 0.422 and 2.639 kg/sec per sterilizer, respectively.

Table 1 shows the results of the thermodynamic states of the steam cogeneration plant and corresponds to Figure 2. The power, steam consumptions and efficiencies

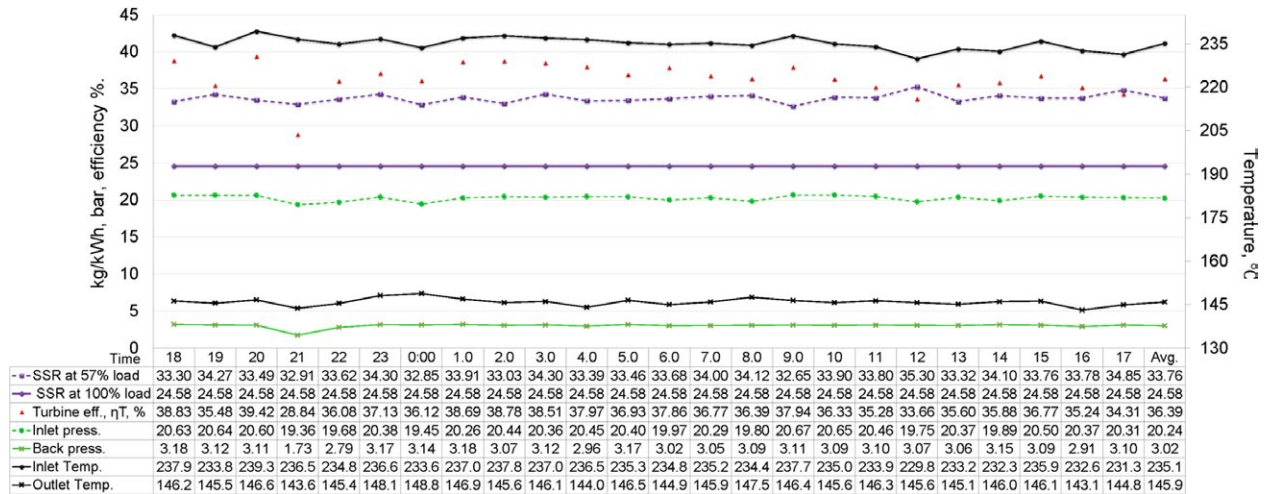


Figure 10. Current steam turbine operation data.

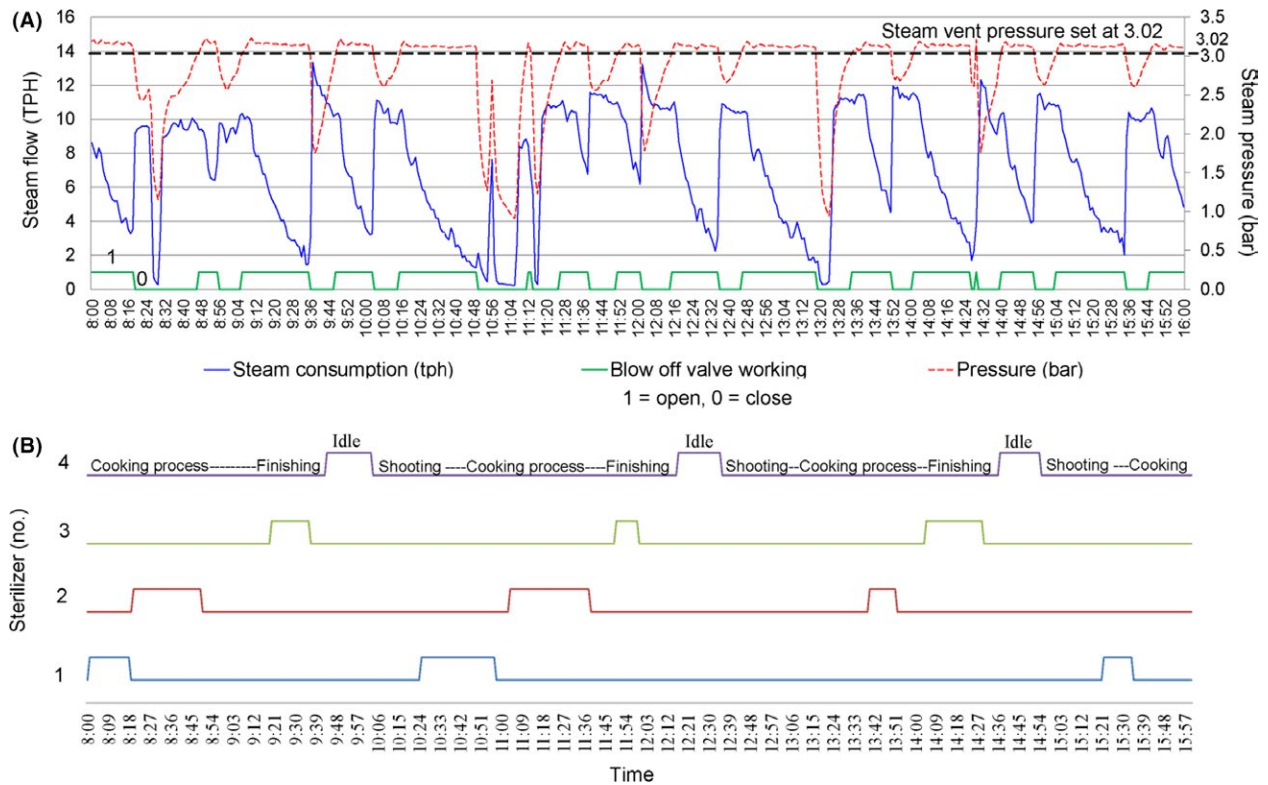


Figure 11. (A) Steam consumption profile of four sterilizers; (B) Operation sequences of the sterilizers.

of the boiler, turbine and cogeneration are also summarized.

Biogas engine power plant efficiency and waste heat potential

The studied POM has used POME as feedstock to produce biogas for use as fuel for the engine power plant, which

normally operates at 1000 kW (94% FL) and exports energy to the grid. Table 2 shows the data collected from the operating engine power plant. The annual power generation is 6,681,962 kWh over 6682 operating hours. The calculated engine electrical efficiency is 38.46% and varies over a standard range (34–40%) [29]. The remaining energy input (61.54%) is rejected as waste heat and other loss. The major sources of waste heat are the engine cooling systems

Table 1. Thermodynamic states of the current cogeneration plant.

State ¹	Description	Phase ²	Mass flow rate (kg/sec) ³	Temperature (°C)	Pressure (MPa)	Enthalpy (kJ/kg)	Energy flow (kW)	Steam turbine loaded (%)	SSR at turbine loaded (kg/kW)	Fractions of steam (kg) and electricity (kW) per tonne FFB	Eff. of boiler, turbine and cogen (%)	Fuel available (kW)
1	Water	Liquid	5.791	95	2.1	399.52	2303.47	–	–	–	–	–
2	Steam	Superheated	5.791	235.14	2.024	2856.25	16540.65	–	–	451.74	72.16	–
3	Steam	Superheated	5.791	145.9	0.302	2742.59	15882.44	–	–	–	–	–
3s	Steam	Wet steam	5.791	143.8	0.302	2545.18	14739.23	–	–	–	–	–
4	Steam	Saturated	4.437	143.8	0.302	2737.85	12148.07	–	–	–	–	–
5	Steam	Saturated	2.104	143.8	0.302	2737.85	5759.46	–	–	164.1	–	–
6	Steam	Saturated	2.334	143.8	0.302	2737.85	6388.78	–	–	182.03	–	–
7	Condensate	Liquid	4.437	100	atm.	418.7	1857.83	–	–	–	–	–
8	Steam	Saturated	1.354	143.8	0.302	2737.85	3706.93	–	–	105.62	–	–
9	Electricity	–	–	–	–	–	658.21	–	–	–	36.54	–
10	Electricity	–	–	–	–	–	617.74	57.2	33.75	13.39	–	–
11	Electricity	–	–	–	–	–	88.05	–	–	–	–	–
12	Electricity	–	–	–	–	–	529.69	–	–	–	36.05	–
13	FFB	Solid	12.819	–	–	–	–	–	–	–	–	–
14	PPF	Solid	1.731	–	–	–	–	–	–	–	–	0
15	FFB	Solid	2.82	–	–	–	20418.81	–	–	–	–	20418.81

¹State numbers correspond to Average Figure 2; State 3s is the isentropic case.

²The phases of state 4, 5, 6, and 8 are assumed as saturated steam due to the steam left the turbine is almost saturated. The phase of state 7 is assumed as saturated liquid.

³The mass flow rate of state 13, FFB is recorded by the factory. The mass flow rate of state 14 (PPF) and 15 (FFB) is calculated by using the RPR of 0.135 and 0.22, respectively.

Table 2. Biogas and power generation of the biogas power plant.

State ¹	13	13	16	17	17 ²	18
	FFB feed (tonne)	Capacity (t/h)	POME generation (m ³)	Biogas production (Nm ³)	Energy input (kWh)	Power generation (kWh)
January	6979	44	5996	2,22,557	12,98,175	4,85,090
February	9489	43	6404	2,59,702	15,14,842	5,53,560
March	18,054	45	8107	2,63,735	15,38,366	4,94,040
April	16,321	43	6828	2,17,856	12,70,754	4,95,400
May	16,075	44	8648	3,04,539	17,76,376	7,18,512
June	21,680	44	7224	2,38,767	13,92,728	5,49,120
July	19,762	44	7056	2,57,939	15,04,558	6,19,830
August	20,990	44	6542	2,27,160	13,25,024	4,89,400
September	18,569	44	6449	2,10,125	12,25,659	4,76,200
October	21,264	44	7672	2,52,352	14,71,969	5,75,700
November	18,217	45	7747	2,30,168	13,42,570	5,47,310
December	13,405	45	7976	2,91,805	17,02,099	6,77,800
Average	16,734	44	7221	2,48,059	14,46,927	5,56,830
Total	2,00,805	–	86,649	29,76,705	3,89,75,884	66,81,962

¹State numbers correspond to Figure 2.

²State numbers 17, energy input is calculated by multiplying the biogas production with biogas LHV.

(LT and HT circuits) and the exhaust gas, other losses, such as radiation and generator and mechanical losses are unavoidable and dissipated. Because the engine operates below its FL, the waste heat generated is reduced accordingly. Therefore, for accuracy, the PAF of the AL was considered along with the heat exchanger effectiveness.

The energy input in Table 3 was calculated from Table 2 (1,000*energy input/power generation) and, to avoid chemical corrosion of the exhaust gas caused by sulfur condensation (130°C dew point), the exhaust gas temperature was limited to 180°C. The actual calculated total waste heat utilization was 984.24 kW, or 37.86% of the energy input, and represented 46.07, 500.38 and 438.79 kW for the LT, HT circuits and the exhaust, respectively, as shown in Table 3. The calculated engine cogeneration efficiency was 76.36% instead of 38.46% (the value of power production only).

Enhanced system

PPF and EFB are major biomass byproducts from the palm oil milling process, which can generate 6.23 and 10.153 t/h of PPF and EFB (at 46.15 t/h FFB capacity, and RPR values of 13.5 and 22%, respectively), or 19729.3 and 20418.81 kW thermal equivalent, respectively. The PPF is primarily used as fuel during CPO production, whereas the EFB is considered for supplemental fuel for power generation when CPO is not being produced. The current plant operation is 4351 h/year; the thermal fuel energy available of the PPF and EFB was calculated as 85.8422 and 88.8422 GWh, respectively.

In the proposed model, the cogeneration plant was designed to operate with or without CPO production. The suitable steam capacity with the CPO production was determined by the CPO process steam consumption, whereas the steam capacity used when CPO is not being produced was calculated from the available fuel (EFB). During CPO production, the designed steam generation was 6.389 kg/sec (23 t/h) at 4.8 MPa and 470°C, and it was supplied to the ECST. The steam consumption during processing was extracted from the extraction side, whereas the remaining steam was passed out through the condensing section to the condenser. The average process steam consumption of this model (4.086 kg/sec) was lower than that of the current system (5.791 kg/sec) because steam was not vented, and steam consumption was reduced by utilizing engine waste heat for FW heating.

The calculated current FW steam consumption was 0.679 kg/sec or 1575.7 kW of heat. Therefore, a certain amount of required heat was replaced by engine waste heat (984.24 kW) (Table 3), and the remainder was balanced by the supplemental steam, which was 0.330 kg/sec (average) or 762.91 kW of heat. The steam recovered from vented steam and engine waste heat utilization was 1.70 kg/sec or 6.14 t/h, and it was used for the power generation. The process steam demands were generated via the heating and sterilization process. The heating process steadily consumes steam, although the sterilization process shows fluctuating demands because of batch processing. Therefore, the maximum, minimum, and average process steam consumption at state 4 varied and were estimated 5.876 kg/sec, 2.201 kg/sec, and 3.991 kg/sec, respectively.

Table 3. Waste heat potential of the 1.063 MW engine-based power plant.

Description	Unit	The engine data		Performance Adjustment factor, PAF	Heat exchanger effectiveness	Calculated data, 94% Actual load	State
		100% (Full load)	75% (Part load)				
Energy input	kW	2658	2047			2598.51	17
Electrical output	kW	1063	796			1000	18
Electrical eff.	%	40	–			38.48	
LT circuit heat	kW	59	39	0.9186	0.85	46.07	19
HT circuit heat	kW	617	499	0.9541	0.85	500.38	20
Exhaust heat (487–180°C)	kW	549	408	0.9382	0.85	437.79	21
Total waste heat	kW					984.24	
Cogeneration eff.	%					76.36	

Because the steam extracted from the turbine is superheated steam, desuperheating water must be injected into the superheated steam to evaporate and create saturated steam. The trial and error method was used to determine the desuperheating water requirement and the steam extraction rate used to balance the extraction steam mass flow rate and the desuperheating water demand, which must be equal to the process steam consumption. The maximum, minimum, and average calculated quantities of injected desuperheating water (state 24) were 0.316, 0.125, and 0.233 kg/sec, respectively; and the maximum, minimum, and average calculated steam extraction rates (state 3) were 5.560, 2.075, and 3.866 kg/sec, respectively.

The power generation (state 9) was estimated to determine the turbine capacity and rating, which were 3,336.69, 4,731.05, and 4,014.47 kW at the maximum, minimum, and average steam extraction rates, respectively. The surplus power that was generated and exported to the grid was 2,834.03 kW (assumed to be 10% of the auxiliary power consumed). The peak power generation occurred when the process steam demand was minimized. Thus, the remaining steam passed through the turbine, where maximum thermal energy was converted to electricity. Therefore, a suitable turbine capacity to handle the peak is 5 MW. The calculated thermal efficiency of the enhanced cogeneration plant was 50.63%, which is higher than that of the current system. PPF was the main fuel used, and it provided slightly less steam than the overall requirement, at 1146.22 kg/h or 3,630.09 kW of heat and was balanced by EFB production, which provided 1.805 t/h or 3,630.09 kW equivalent. Therefore, the remaining EFB was equal to 8.35 t/h, 36,330.85 t/year or 73.05 GWh of thermal energy, and this energy is planned for use when CPO is not being produced. Table 4 shows the results of the thermodynamic states of the proposed model with the CPO production.

When CPO is not being produced, the cogeneration plant still operates continuously, although it is only used for power generation because of the lack process steam

demand, and the collected EFB is used as fuel to run the cogeneration plant in this mode. If the operating time of the cogeneration plant is assumed to be 7500 h/year, then the plant operating hours without CPO production are 3149 h/year (7,500–4,351 h). Based on the collected EFB (73.05 GWh thermal) and the 80% boiler efficiency, the calculated steam capacity is 21.038 t/h (5.844 kg/sec) for power generation. Because process steam is not required, most of the steam is supplied to the turbine and dedicated to power generation. The calculated power generation was 5,040.33 kW at the generator output, and 4,223.29 kW of which is exported to the grid. The calculated thermal efficiency of the power plant was 19.77%, and the large thermal energy loss was as high as 67% of the energy input, which is rejected into the condenser (state 32). The LT circuit heat is not fully utilized in this mode because of the low FW requirement, and it was calculated as 10 kW (at 50°C, FW outlet temperature). Table 5 shows the results of the thermodynamic states of the power generation model when CPO is not being produced. The total increased power generation was 25.63 GWh per year in the studied case. Nationwide, this value was estimated to reach 1384 GWh based on FFB production of 12 MMT/year, and 90% is consumed by wet POMs, with 54 POMs operating for 4351 h at 46.15 t/h FFB (the same as the considered case). The carbon dioxide emissions were reduced by 0.66 million metric tonnes of carbon dioxide equivalent (MMTCO) based on 0.477 kg CO₂/kWh in 2017.

Technical barriers and the energy policies

Because CPO production is a seasonal production process, it depends on the cultivation season. Typically, high output starts from March to November and declines from December to February (Table 2). An average production rate is 4351 h a year, which means almost half of the year is idle. The traditional cogeneration plant design disregards energy efficiency and ties the palm oil

Table 4. Results of thermodynamic states of the enhanced cogeneration model (with CPO production).

State ¹	Description	Phase	Mass flow rate (kg/sec)	Temperature (°C)	Pressure (MPa)	Enthalpy (kJ/kg)	Energy flow (kW)	Thermal efficiency (%)	SSR of turbine (kg/kW)	Fuel available (kW)
1	Water	Liquid	6.389	105	5.1	440.46	2814.05	-	-	-
2	Steam	Superheated	6.389	470	4.8	3365.44	21501.42	-	-	-
3 (max.)	Steam	Superheated	5.56	216.5	0.3	2895.09	16096.67	-	-	-
3 (min.)	Steam	Superheated	2.075	216.5	0.3	2895.09	6007.3	-	-	-
3 (avg.)	Steam	Superheated	3.866	216.5	0.3	2895.09	11192.4	-	-	-
3s	Steam	Superheated	5.56	143.92	0.3	2738.3	15224.95	-	-	-
4 (max.)	Steam	Saturated	5.876	143.8	0.3	2737.85	16086.71	-	-	-
4 (min.)	Steam	Saturated	2.201	143.8	0.3	2737.85	6026.72	-	-	-
4 (avg.)	Steam	Saturated	3.991	143.8	0.3	2737.85	10925.88	-	-	-
5 (max.)	Steam	Saturated	3.906	143.8	0.3	2737.85	10692.83	-	-	-
5 (min.)	Steam	Saturated	0.422	143.8	0.3	2737.85	1155.98	-	-	-
5 (avg.)	Steam	Saturated	2.104	143.8	0.3	2737.85	5759.46	-	-	-
6	Steam	Saturated	1.654	143.8	0.3	2737.85	4528.18	-	-	-
7	Condensate	Liquid	5.876	100	atm.	419	2461.91	-	-	-
8	Steam	Saturated	-	-	-	-	-	-	-	-
9 (max.)	Electricity	-	-	-	-	-	3336.69	-	6.89	-
9 (min.)	Electricity	-	-	-	-	-	4731.05	-	4.86	-
9 (avg.)	Electricity	-	-	-	-	-	4014.47	-	5.73	-
10 (avg.)	Electricity	-	-	-	-	-	3737.47	-	-	-
11 (avg.)	Electricity	-	-	-	-	-	373.75	-	-	-
12 (avg.)	Electricity	-	-	-	-	-	529.69	-	-	-
13	FFB	Solid	12.82	-	-	-	-	-	-	-
14	PPF	Solid	1.731	-	-	-	19729.13	-	-	-3630.09
15	EFB	Solid	2.82	-	-	-	20418.81	50.63	-	16788.72
16	POME	Liquid	-	-	-	-	-	-	-	-
17	Biogas	Gas	-	-	-	-	2599	-	-	-
18	Electricity	-	-	-	-	-	1000	-	-	-
19	Heat, LT	Liquid	-	-	-	-	46.07	-	-	-
20	Heat, HT	Liquid	-	-	-	-	500.38	-	-	-
21	Heat, exh.	Gas	-	-	-	-	437.79	-	-	-
22 (max.)	Water	Liquid	5.56	30	0.3	126.02	700.67	-	-	-
22 (min.)	Water	Liquid	2.075	30	0.3	126.02	261.49	-	-	-
22 (avg.)	Water	Liquid	3.866	30	0.3	126.02	487.19	-	-	-
23 (avg.)	Water	Liquid	6.389	105	0.1	440.23	2812.58	-	-	-
24 (max.)	Water	Liquid	0.316	30	5.1	130.3	41.2	-	-	-
24 (min.)	Water	Liquid	0.125	30	5.1	130.3	16.3	-	-	-
24 (avg.)	Water	Liquid	0.233	30	5.1	130.3	30.37	-	-	-
25 (min.)	Steam	Wet 4.39%	0.829	53.99	-0.086	2494.98	2068.06	-	-	-
25 (max.)	Steam	Wet 4.39%	4.314	53.99	-0.086	2494.98	10763.07	-	-	-

(Continues)

Table 4 (Continued)

State ¹	Description	Phase	Mass flow rate (kg/sec)	Temperature (°C)	Pressure (MPa)	Enthalpy (kJ/kg)	Energy flow (kW)	Thermal efficiency (%)	SSR of turbine (kg/kW)	Fuel available (kW)
25 (avg.)	Steam	Wet 4.39%	2.523	53.99	-0.086	2494.98	6294.56	-	-	-
25s	Steam	Wet 15.35%	2.523	53.99	-0.086	2234.98	5638.6	-	-	-
26 (avg.)	Condensate	Liquid	2.523	54	-0.086	225.97	570.1	-	-	-
27 (min.)	Condensate	Liquid	0.829	54	0.3	226.3	187.58	-	-	-
27 (max.)	Condensate	Liquid	4.314	54	0.3	226.3	976.23	-	-	-
27 (avg.)	Condensate	Liquid	2.523	54	0.3	226.3	570.93	-	-	-
28 (max.)	Steam	Saturated	0.404	143.8	0.3	2737.85	1106.97	-	-	-
28 (min.)	Steam	Saturated	0.253	143.8	0.3	2737.85	693.49	-	-	-
28 (avg.)	Steam	Saturated	0.331	143.8	0.3	2737.85	905.99	-	-	-
29 (avg.)	Condensate	Liquid	0.331	100	atm.	419	138.65	-	-	-
30 (avg.)	Electricity	-	-	-	-	-	3363.72	-	-	-
31 (avg.)	Electricity	-	-	-	-	-	2834.03	-	-	-
32 (avg.)	Heat (loss)	-	-	-	-	-	5724.46	-	-	-

¹State numbers correspond to Figure 7; State 3s and 25s are the isentropic case; State 11, the auxiliaries power consumption is assumed 10% of the generator output.

milling process and the cogeneration plant operation together. Specifically, the cogeneration plant is always in operation during CPO production, a period when bio-energy byproducts are generated in large quantities that exceeded the factory demand, which leads to their subsequent waste.

Currently, the country's energy policies, including Thailand PDP 2015, AEDP 2015 and EEDP 2015, have been adjusted to achieve a national sustainability goal [33, 34]. These plans are related to waste energy utilization, energy conservation, and energy-efficiency enhancement based on the various subsidies. These programs empower and could change the POM owners traditional attitude, and the proposed model could be used to overcome the constraints mentioned above. Nevertheless, the capability of the nation's grid connection is a critical factor for success that needs further support.

Although the ECST can manage a wide range of steam operations, sterilization steam fluctuations may affect the turbine control. Thus, a suitably sized steam accumulator may reduce the pressure fluctuations [23]. High-efficiency boilers, EFB preparation, and combustion technology, such as fluidized bed combustion, are also technical issues that need consideration because many chemical compositions contained in the EFB may create clinker, fouling, and corrosion when fired. However, boiler manufacturers and researchers have studied and solved this type of problem [35, 36]. Moreover, engine-based cogeneration plants must perform according to the engine manufacturer specification, particularly the cooling temperature and exhaust gas back pressure. Accordingly, developing the human resources for sustainability schemes is an essential component.

Conclusions

In this paper, the cogeneration efficiency enhancement and integrated waste energy utilization in the POMs were demonstrated using a standard 45 t/h FFB POM as a case study. The significant lost energy, vented sterilization steam, engine waste heat, and EFB biomass fuel have been recovered, utilized, and harnessed by the proposed cogeneration model. A thermodynamic analysis based on the first law of thermodynamics was conducted. The proposed model shows that the surplus power could generate 2.834 and 4.223 MW with and without CPO production, respectively, or 1384 GWh for the country, thereby reducing carbon dioxide emissions by 0.66 MMTCO. In addition to the surplus power production, the cogeneration plant can operate continuously and extend its operation to 7500 h/year instead of the current intermittent 4351 h. Increasing the energy efficiency by utilizing the waste energy promotes sustainability and economical and

Table 5. Results of thermodynamic states of the enhanced cogeneration model (without CPO production).

State ¹	Description	Phase	Mass flow rate (kg/sec)	Temperature (°C)	Pressure (MPa)	Enthalpy (kJ/kg)	Energy flow (kW)	Thermal efficiency (%)	SSR of turbine (kg/kW)	Fuel available (kW)
1	Water	Liquid	5.844	105	5.1	440.46	2573.93	-	-	-
2	Steam	Superheated	5.844	470	4.8	3365.44	19666.74	-	-	-
3 (max.)	Steam	Superheated	-	-	-	-	-	-	-	-
3 (min.)	Steam	Superheated	-	-	-	-	-	-	-	-
3 (avg.)	Steam	Superheated	0.116	216.5	0.3	2895.09	335.83	-	-	-
3s	Steam	Superheated	0.116	143.92	0.3	2738.3	317.64	-	-	-
4 (max.)	Steam	Saturated	-	-	-	-	-	-	-	-
4 (min.)	Steam	Saturated	-	-	-	-	-	-	-	-
4 (avg.)	Steam	Saturated	0.123	143.8	0.3	2737.85	336.74	-	-	-
5 (max.)	Steam	Saturated	-	-	-	-	-	-	-	-
5 (min.)	Steam	Saturated	-	-	-	-	-	-	-	-
5 (avg.)	Steam	Saturated	-	-	-	-	-	-	-	-
6	Steam	Saturated	-	-	-	-	-	-	-	-
7	Condensate	Liquid	-	-	-	-	-	-	-	-
8	Steam	Saturated	-	-	-	-	-	-	-	-
9 (max.)	Electricity	-	-	-	-	-	-	-	-	-
9 (min.)	Electricity	-	-	-	-	-	-	-	-	-
9 (avg.)	Electricity	-	-	-	-	-	-	-	4.17	-
10 (avg.)	Electricity	-	-	-	-	-	5040.33	-	-	-
11 (avg.)	Electricity	-	-	-	-	-	4692.54	-	-	-
12 (avg.)	Electricity	-	-	-	-	-	469.25	-	-	-
13	FFB	Solid	-	-	-	-	0	-	-	-
14	PPF	Solid	-	-	-	-	-	-	-	-
15	EFB	Solid	2.951	-	-	-	21366.01	19.77	-	21365.9
16	POME	Liquid	-	-	-	-	-	-	-	-
17	Biogas	Gas	-	-	-	-	2599	-	-	-
18	Electricity	-	-	-	-	-	1000	-	-	-
19	LT, heat	Liquid	-	-	-	-	10	-	-	-
20	HT, heat	Liquid	-	-	-	-	500.38	-	-	-
21	Exh., heat	Gas	-	-	-	-	437.79	-	-	-
22	Water	Liquid	0.116	30	0.3	126.02	14.62	-	-	-
23	Water	Liquid	5.844	105	0.1	440.23	2572.59	-	-	-
24 (max.)	Water	Liquid	-	-	-	-	-	-	-	-
24 (min.)	Water	Liquid	-	-	-	-	-	-	-	-
24 (avg.)	Water	Liquid	0.007	30	5.1	130.3	0.91	-	-	-
25 (max.)	Steam	-	-	-	-	-	-	-	-	-
25 (min.)	Steam	-	-	-	-	-	-	-	-	-
25 (avg.)	Steam	Wet 4.39%	5.728	53.99	-0.086	2494.98	14290.59	-	-	-
25s	Steam	Wet 15.35%	5.728	53.99	-0.086	2234.98	12801.36	-	-	-

(Continues)

Table 5 (Continued)

State ¹	Description	Phase	Mass flow rate (kg/sec)	Temperature (°C)	Pressure (MPa)	Enthalpy (kJ/kg)	Energy flow (kW)	Thermal efficiency (%)	SSR of turbine (kg/kW)	Fuel available (kW)
26	Condensate	Liquid	5.728	54	-0.086	225.97	1294.3	-	-	-
27	Condensate	Liquid	5.728	54	0.3	226.3	1296.19	-	-	-
28	Steam	Saturated	0.123	143.8	0.3	2737.85	336.97	-	-	-
29	Condensate	Liquid	0.123	100	atm.	149	18.34	-	-	-
30 (avg.)	Electricity	-	-	-	-	-	4223.29	-	-	-
31 (avg.)	Electricity	-	-	-	-	-	4223.29	-	-	-
32 (avg.)	Heat (loss)	-	-	-	-	-	12996.29	-	-	-

¹State numbers correspond to Figure 7; State 3s and 25s are the isentropic case; State 11, the auxiliaries power consumption is assumed 10% of the generator output.

industrial competitiveness and should be implemented in POMs nationwide and in other palm oil-producing countries. Although the study shows increased power generation and extended operating hours of the cogeneration plant in POMs, seasonal change effect of the intermittent operation of the palm oil milling process. Therefore, to investigate this problem, using optimization methods is one of the options for further study.

Conflicts of Interest

None declared.

References

1. Palm Oil | Global Palm Oil Production. 2016/2017. Available at www.globalpalmoilproduction.com/ (accessed October 2016)
2. Prasertsan, S., and P. Prasertsan. 1996. Biomass residues From Palm Oil Mills in Thailand : an overview on quantity and potential usage. *Biomass Bioenergy*. 11:387–395.
3. Ohimain, E. I., and S. C. Izah. 2015. Energy self-sufficiency of semi-mechanized oil palm Processing: A case study of Bayelsa palm mill, Elebele, Nigeria. *Energy Econ. Lett.* 2:35–45.
4. Agricultural statistics of Thailand (OAE). 2016. Available at <http://www.oae.go.th/download/journal/trends2558.pdf>. (accessed May 2016)
5. Department of Alternative Energy Development and Efficiency (DEDE), Empty Fruit Bunch. 2016. Available at <http://webkc.dede.go.th/testmax/node/2529> (accessed May 2016)
6. Viramuthu, V. 2010. The potential usage of oil palm biomass for the potential of energy with sampling and Malaysian case study. Lambert Academic, Lexington, KY.
7. Bazmi, A. A., G. Zahedi, and H. Hashim. 2011. Progresses and challenges in Utilization of palm oil biomass as fuel for decentralized electricity generation. *Renew. Sustain. Energy Rev.* 15:574–583.
8. Mahlia, T. M. I., J. H. Yong, A. Safari, and S. Mekhilef. 2012. Techno-economic analysis of palm oil mill wastes to generate power for grid-connected utilization. *Energy Educ. Sci. Technol. A Energy Sci. Res.* 28:1117–1136.
9. Sungkaew, W. 2015. Potential of oil palm biomass residues for electricity generation in Southern Thailand. M.Eng. thesis, Prince of Songkla University, Thailand. Available at <http://kb.psu.ac.th:8080/psukb/bitstream/2016/10439/1/404545.pdf> (accessed June 2017)
10. Harsono, S. S., P. Grundmann, and S. Soebronto. 2014. Anaerobic treatment of palm oil mill effluents: potential contribution to net energy yield and reduction of

- greenhouse gas emissions from biodiesel production. *J. Clean. Prod.* 6:619–627.
11. Hosseini, S. E., and M. Abdul Wahid. 2013. Feasibility study of biogas production and utilization as a source of renewable energy in Malaysia. *Renew. Sustain. Energy Rev.* 19:454–462.
 12. Begun, S., M. Firdaus, and M. Saad. 2013. Techno-economic analysis of electricity generation from biogas using palm oil waste. *Asian J. Sci. Res.* 6:290–298.
 13. Prasertsan, S., and B. Sujakulnukij. 2006. Biomass and biogas energy in Thailand: potential, opportunities and barriers. *Renewable Energy* 31:599–610.
 14. Ohimain, E. I., and S. C. Izah. 2014. Estimation of potential electrical energy and currency equivalent from un-tapped palm oil mill effluents in Nigeria. *Int. J. Farm. Allied Sci.* 3:855–862.
 15. Pattanapongchai, A., and B. Limmeechokchai. 2014. The co-benefits of biogas from the palm oil industry in long-term energy planning: a least-cost biogas upgrade in Thailand. *Energy Source, Part B* 9:360–373.
 16. Energy for Environment Foundation (EFE). 2015. Available at www.efo.or.th/datacenter/ckupload/files/EFE%20LAY4.pdf; (accessed May 2015)
 17. Booneimsri, P., K. Kubaha, and C. Chullbodhi. 2016. Waste heat potential assessment of the engine based power plant in Thai palm oil mills, International conference on sustainable energy and engineering application ICSEEA 2016, Jakarta Indonesia.
 18. Yusoff, S. 2006. Renewable energy from palm oil-innovation on effective utilization waste. *Clea. Prod.* 14:87–93.
 19. Wibulsawas, P., and W. Tia. 1992. Potential of cogeneration in Thai palm oil mills. *Res. Develop. J. Eng. Institute Thailand* 3:48–55.
 20. Nasrin, A. B., N. Ravi, W. S. Lim, Y. M. Choo, and A. M. Fadzil. 2011. Assessment of the performance and potential export renewable energy (RE) from typical cogeneration plants used in palm oil mills. *J. Eng. Appl. Sci.* 6:433–439.
 21. Husain, Z., Z. A. Zainal, and M. Z. Abdullah. 2003. Analysis of biomass-residue-based cogeneration system in palm oil mills. *Biomass Bioenerg.* 24:117–124.
 22. Aziz, M., and T. Kurniawan. 2016. Enhanced utilization of palm oil mill wastes for power generation. *Chem. Eng. Transaction* 52:727–732.
 23. Mohd. Halim Shah, I., A. A. Mustafa Kamal, and M. Nor Azim. 2009. Research work on steam accumulator in palm oil mill. *Eur. J. Sci. Res.* 37:628–640.
 24. Mohd. Halim Shah, I., A. A. Mustafa Kamal, and M. Nor Azim. 2009. A system approach to mathematical modelling for steam accumulator in palm oil mill. *Eur. J. Sci. Res.* 35:544–558.
 25. Aziz, M., T. Oda, and T. Kashiwagi. 2015. Innovatives steam drying of empty fruit bunch with high energy efficiency. *Drying Technol.* 33:395–405.
 26. Thailand power development plan. Available at <http://www.eppo.go.th/index.php/en/policy-and-plan/en-tieb/tieb-pdp> (accessed January 2017)
 27. Thailand submits NAMA –UNFCCC newsroom. Available at <http://newsroom.unfccc.int/unfccc-newsroom/thailand-submits-nama/> (accessed January 2017)
 28. Biomass Database Potential in Thailand. Available at <http://weben.dede.go.th/webmax/content/biomass-database-potential-thailand> (accessed June 2016)
 29. Deublein, D., and A. Steinhauser. 2008. Biogas from waste and renewable resources, Germany. WILEY-VCH. pp. 51–55, 367.
 30. Cengel, Y. A., and M. A. Boles. 1994. *Thermodynamics: An engineering approach*. 2nd ed. Pp. 529–531. McGraw-Hill Inc, New York, NY.
 31. Blocl, H. P. 1995. *A practical guide to steam turbine technology*. Pp. 304–305. McGraw-Hill, New York, NY.
 32. Breeze, P. 2015. *Power generation technology*. 2nd ed. Pp. 98–99. Newnes-Elsevier, Waltham, MA 02451, USA.
 33. Rosen, M. A., and S. Koochi-Fayegh. 2016. *Cogeneration and district energy systems*. Pp. 10–11. The Institute of Engineering and Technology, London, U.K.
 34. Petchers, N. 2003. *Combined heating, cooling & power handbook, An integrated approach to energy resource optimization*. Pp. 167–170. The Fairmont Press, Inc, New York, NY.
 35. Efficient combuston of empty fruit bunch (FB). Available at <http://pennwell.sds06.websds.net/2014/kl/rewa/papers/T1S1O2-paper.pdf> (accessed September 2017)
 36. Program exploration of Indonesian State palm. Available at <http://www.nedo.go.jp/content/100494437.pdf> (accessed August 2017)